

## Short-range order in amorphous SiO<sub>x</sub> by x ray photoelectron spectroscopy

Yu. N. Novikov and V. A. Gritsenko

Citation: *J. Appl. Phys.* **110**, 014107 (2011); doi: 10.1063/1.3606422

View online: <http://dx.doi.org/10.1063/1.3606422>

View Table of Contents: <http://jap.aip.org/resource/1/JAPIAU/v110/i1>

Published by the [American Institute of Physics](#).

---

### Related Articles

Pressure induced amorphization of ZrMo<sub>2</sub>O<sub>8</sub> and its relaxation on decompression as seen by in situ total x-ray scattering

*J. Appl. Phys.* **112**, 023511 (2012)

Optical switching and related structural properties of epitaxial Ge<sub>2</sub>Sb<sub>2</sub>Te<sub>5</sub> films

*J. Appl. Phys.* **111**, 113524 (2012)

Structure of iron nanolayers embedded in amorphous alloys

*Appl. Phys. Lett.* **100**, 203108 (2012)

Possible frictionless transport of amorphous matter in confined microdomains

*J. Appl. Phys.* **111**, 093531 (2012)

Amorphization and amorphous stability of Bi<sub>2</sub>Te<sub>3</sub> chalcogenide films

*Appl. Phys. Lett.* **100**, 142114 (2012)

---

### Additional information on *J. Appl. Phys.*


Journal Homepage: <http://jap.aip.org/>

Journal Information: [http://jap.aip.org/about/about\\_the\\_journal](http://jap.aip.org/about/about_the_journal)

Top downloads: [http://jap.aip.org/features/most\\_downloaded](http://jap.aip.org/features/most_downloaded)

Information for Authors: <http://jap.aip.org/authors>

## ADVERTISEMENT



Special Topic Section:  
**PHYSICS OF CANCER**

Why cancer? Why physics? [View Articles Now](#)

## Short-range order in amorphous SiO<sub>x</sub> by x ray photoelectron spectroscopy

Yu. N. Novikov<sup>a)</sup> and V. A. Gritsenko*Institute of Semiconductor Physics, Novosibirsk 630090, Russia*

(Received 25 April 2011; accepted 25 May 2011; published online 11 July 2011)

The Si 2p x ray photoelectron spectra of SiO<sub>x</sub> with a different composition of  $0 \leq x \leq 2$  have been studied experimentally and theoretically. The SiO<sub>x</sub> films were prepared by low-pressure chemical vapor deposition from SiH<sub>4</sub> and N<sub>2</sub>O source at 750 °C. Neither random bonding nor random mixture models can adequately describe the structure of these compounds. The interpretation of the experimental results is discussed according to a large scale potential fluctuation due to the spatial variation of chemical composition in SiO<sub>x</sub>. © 2011 American Institute of Physics.

[doi:10.1063/1.3606422]

### I. INTRODUCTION

The SiO<sub>x</sub> ( $0 \leq x \leq 2$ ) and SiN<sub>x</sub> ( $0 \leq x \leq 4/3$ ) are two key dielectrics in silicon devices. *Non-stoichiometric* compounds of SiO<sub>x</sub> are an active research subject due to their potential applications in the development of light emitting devices,<sup>1</sup> light-absorbing layer on the screen,<sup>2</sup> solar cell,<sup>3</sup> and storage layer in the flash memory.<sup>4</sup>

SiO<sub>x</sub> consists of Si—Si and Si—O bonds. The short-range order in tetrahedral solids, such as SiO<sub>x</sub>, is described by the Mott rule.<sup>5</sup> In these compounds, the silicon atom is coordinated by four O or Si atoms and the O atom is coordinated by two Si atoms. The atomic and electronic structure of SiO<sub>x</sub> was studied by photoelectron spectroscopy,<sup>6</sup> high-resolution transmission electron microscopy,<sup>6</sup> secondary ion mass spectrometry,<sup>6</sup> photoemission spectroscopy,<sup>7</sup> infrared spectroscopy,<sup>8</sup> optical methods,<sup>9</sup> and electron paramagnetic resonance.<sup>10</sup> Nevertheless, there is no universal model for SiO<sub>x</sub> electron structure. The aim of this work is an experimental investigation of SiO<sub>x</sub> electronic structure using high-resolution x ray photoelectron spectroscopy (XPS). The random bonding (RB) and random mixture (RM) models<sup>5–7,11</sup> are used to describe the short range order in SiO<sub>x</sub>. The intermediate model (IM) is suggested and discussed to describe the short-range order and electronic structure of SiO<sub>x</sub>.

### II. SAMPLES PREPARATION AND MEASUREMENT

The SiO<sub>x</sub> with thicknesses  $\approx 20$  nm and a different composition of  $0 \leq x \leq 2$  was prepared on silicon n-type (100) substrates (resistivity  $\approx 10$  ohm-cm) by low-pressure chemical vapor deposition (LP CVD) from the SiH<sub>4</sub> and N<sub>2</sub>O source at 750 °C. The SiO<sub>x</sub> stoichiometry layers ( $x = [O]/[Si]$ ) were changed by modifying the pressure ratios of SiH<sub>4</sub> gas. Ellipsometry was employed to measure SiO<sub>x</sub> thicknesses.

XPS measurements were performed in the Kratos AXIS-HS system using a source of monochromatic Al K x ray radiation of  $h\nu = 1486.6$  eV. The natural oxide film from the samples was removed by 2-min etching in an HF-methanol mixture (1:30). The binding energies were measured related to the 1s

peak of carbon in cyclohexane with binding energy 285.0 eV. In cases of significant positive charging of a sample, the charge was compensated using a beam of low-energy electrons. All the XPS measurements were performed for the sample surface oriented perpendicularly to the electron energy analyzer axis (zero polar angle).

### III. THEORETICAL MODELS

The experimental spectra are compared to theoretical calculations based on RB and RM models. According to the RB model, a SiO<sub>x</sub> is composed of five types of tetrahedrons SiO<sub>ν</sub>Si<sub>(4-ν)</sub> (where  $\nu = 0, 1, 2, 3,$  and  $4$ ). The RB model assumes the absence of point defects, such as dangling bond  $\equiv \text{Si}\bullet$ ,  $-\text{O}\bullet$  in SiO<sub>x</sub> (here, symbols “—” and “•” denote a covalent bond and unpaired electron, respectively). The intensities from SiSi<sub>4</sub>, SiSi<sub>3</sub>O, SiSi<sub>2</sub>O<sub>2</sub>, SiSiO<sub>3</sub>, and SiO<sub>4</sub> tetrahedrons were widened with Gaussian function. To describe the experimental spectra using RB and RM models, we need to know the peak position (PP), distribution function (intensities), and full width at half maximum (FWHM) for the five and two tetrahedrons, respectively. The distributions function of the SiO<sub>ν</sub>Si<sub>(4-ν)</sub> tetrahedrons in the RB model is described by

$$I_{\nu}(x) = \left(\frac{x}{2}\right)^{\nu} \left(1 - \frac{x}{2}\right)^{4-\nu} \frac{4!}{\nu!(4-\nu)!}. \quad (1)$$

According to the RM model, an x ray photoelectron Si 2p spectrum should have two components corresponding to the a—Si (SiSi<sub>4</sub> tetrahedron) and a—SiO<sub>2</sub> (SiO<sub>4</sub> tetrahedron) phases, respectively. The spectra intensities in the RM model from SiSi<sub>4</sub> and SiO<sub>4</sub> tetrahedrons are  $I_0(x) = (1-x/2)$  and  $I_4(x) = (x/2)$ , respectively.

The composition  $x$  of the experimental samples was estimated according to the formula<sup>7</sup>

$$x = \frac{1 \sum_{\nu=1}^4 \nu I_{\nu}}{2 \sum_{\nu=0}^4 I_{\nu}}. \quad (2)$$

Here, as for the above mentioned RB model, it was suggested that SiO<sub>x</sub> is composed of five types of tetrahedrons

<sup>a)</sup>Author to whom correspondence should be addressed. Electronic mail: nov@isp.nsc.ru.

$\text{SiO}_\nu\text{Si}_{(4-\nu)}$  (where  $\nu=0, 1, 2, 3$ , and  $4$ ). The distributions function  $I_\nu$  of the  $\text{SiO}_\nu\text{Si}_{(4-\nu)}$  tetrahedrons, in general case, is not described by the RB model, but it is determined according to the conditions of synthesis. The intensities ( $I_\nu$ ) from five tetrahedrons were determined from the best agreement between experimental spectra and the calculated one (using Newton method). As for the RB model, PP and FWHM were used.

#### IV. EXPERIMENTAL AND CALCULATED RESULTS

The Si 2p experimental PP (Fig. 1) of a-SiO<sub>2</sub> is  $E_0 = 103.5$  eV and FWHM is  $\sigma_0 = 1.2$  eV. The Si 2p experimental PP (Fig. 1) of a-Si is  $E_4 = 99.5$  eV and FWHM is  $\sigma_4 = 0.6$  eV. These were experimentally found values of PP and FWHM for SiSi<sub>4</sub> and SiO<sub>4</sub> tetrahedrons were used in the calculation. The FWHM and PP for SiSiO<sub>3</sub>, SiSi<sub>2</sub>O<sub>2</sub>, and SiSi<sub>3</sub>O tetrahedrons were estimated based on the linear interpolation of values  $E_0$ ,  $E_4$ ,  $\sigma_0$ , and  $\sigma_4$  using the number of oxygen atoms as a parameter.<sup>11</sup>

Figure 1 shows the results of calculations for the determination of SiO<sub>x</sub> composition. The fitting of experimental data resulted in the calculating composition of SiO<sub>x</sub> layers:  $x=0, 0.7, 0.98, 1.47$ , and  $2.0$ . The calculation indicates the existence of silicon phase in SiO<sub>x</sub> for  $x < 2$ .

Figure 2 shows the experimental x ray photoelectron Si 2p spectra of SiO<sub>x</sub> with different compositions (in bold lines) and the calculated one according to the RB model (in dashed line). The RB calculation predicts that the Si 2p spectrum consists of a single broad peak and does not agree to the corresponding experimental spectrum. According to the RB

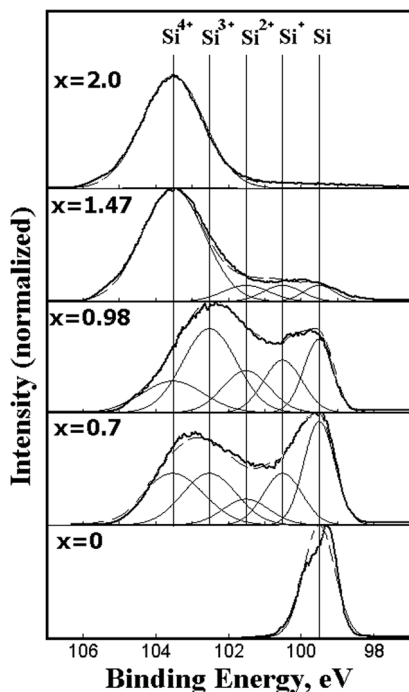


FIG. 1. XPS spectra of Si 2p levels in SiO<sub>x</sub> samples of various compositions. The experimental spectra are shown in bold lines. The results for determination (upper left) of SiO<sub>x</sub> composition are shown with a dashed line. The intensities from SiSi<sub>4</sub>, SiSi<sub>3</sub>O, SiSi<sub>2</sub>O<sub>2</sub>, SiSiO<sub>3</sub>, and SiO<sub>4</sub> tetrahedrons are marked with Si, Si<sup>+</sup>, Si<sup>2+</sup>, Si<sup>3+</sup>, and Si<sup>4+</sup>, respectively.

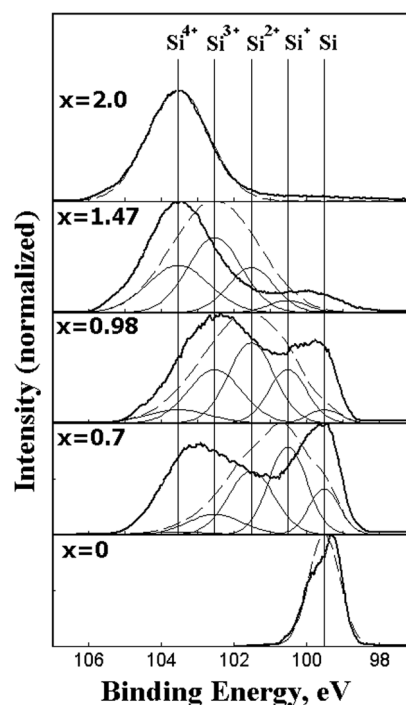


FIG. 2. XPS spectra of Si 2p levels in SiO<sub>x</sub> samples of various compositions. The experimental spectra are shown in bold lines. The results of theoretical calculations according to the RB model are shown with a dashed line. The intensities from SiSi<sub>4</sub>, SiSi<sub>3</sub>O, SiSi<sub>2</sub>O<sub>2</sub>, SiSiO<sub>3</sub>, and SiO<sub>4</sub> tetrahedrons are marked with Si, Si<sup>+</sup>, Si<sup>2+</sup>, Si<sup>3+</sup>, and Si<sup>4+</sup>, respectively.

model, the peak position shifts toward low binding energies with a decreasing oxygen content in SiO<sub>x</sub>. The RB model underestimates the role of SiSi<sub>4</sub> and SiO<sub>4</sub> tetrahedrons for SiO<sub>x</sub> ( $x=0.7, 0.98, 1.47$ ). The RB model predicts the deficiency of silicon phase, which is presented in the experimental spectrum for  $x < 2$ . Thereby, SiO<sub>x</sub> consists of five sorts of tetrahedrons, but the probability to find tetrahedrons is not described by the RB model.

The simulations results of the XPS spectra of SiO<sub>x</sub> within the framework of the RM are presented with the dashed line in Fig. 3. According to the RM model, the Si 2p spectrum has two peaks corresponding to Si and SiO<sub>2</sub> phases, which correlate with the experimental spectrum in the peak locations. The experimental XPS shows the existence of different chemical phases in SiO<sub>x</sub> corresponding to SiSiO<sub>3</sub>, SiSi<sub>2</sub>O<sub>2</sub>, and SiSi<sub>3</sub>O tetrahedral, which are not described by the RM mode. As, for example, for SiO<sub>0.98</sub>, the calculated XPS spectra predict the existence of a SiO<sub>2</sub> component, which does not exist in experimental spectra (Fig. 3).

Thereby, it was found that both models (RB and RM) cannot quantitatively describe the experimental Si 2p spectra of SiO<sub>x</sub>. Also, the figures (2 and 3) show that experimental x ray photoelectron Si 2p spectra cannot be described by a simple summation of RB and RM spectra with definite proportions. For example, it is clear for  $x=0.7$ .

#### V. DISCUSSION

As a rule, at low temperature (less than 300 K) of samples preparation, the RB model describes the experimental results. At high temperatures of preparation of samples SiO<sub>x</sub>,

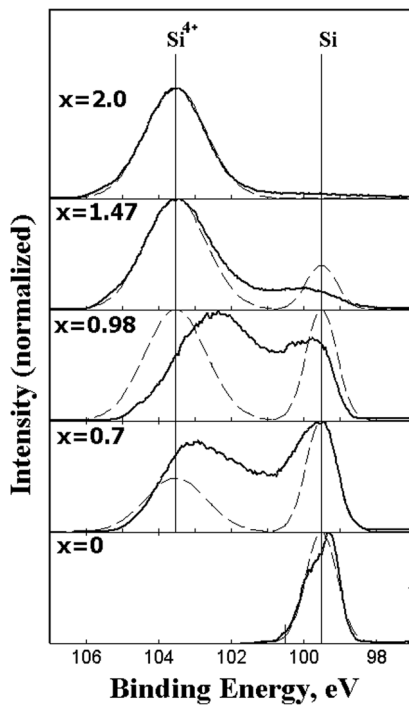


FIG. 3. XPS spectra of Si 2p levels in  $\text{SiO}_x$  samples of various compositions. The experimental spectra are shown in bold lines. The results of theoretical calculations according to the RM model are shown with a dashed line. The intensities from  $\text{SiSi}_4$  and  $\text{SiO}_4$  tetrahedrons are marked with Si and  $\text{Si}^{4+}$ , respectively.

the experimental results are better described by the RM model. For example, previously, it was found<sup>6</sup> that  $\text{SiO}_x$  deposited at 660 °C consists of a nanometer-scale mixture containing Si,  $\text{SiO}_2$ , and suboxide  $\text{SiO}_{0.86}$ . In the paper,<sup>8</sup> the  $\text{SiO}_x\text{:H}$  samples were deposited at 225 °C. It was shown by infrared absorption that the experimental results are described by the RB model. In Ref. 7, the photoemission measurements of  $\text{SiO}_x$  ( $0 \leq x \leq 2$ ) were presented. It was found that the concentration of Si—Si and Si—O bonds are essentially in agreement with the RB model. However, for oxygen- and silicon-rich phases, it is also evident at intermediate stoichiometries. Since  $\text{SiO}_x$  is synthesized under thermodynamically nonequilibrium conditions, the product structure depends on the method of synthesis. In particular, provided that the chemical composition is the same, the optical bandgap width, for example, in  $\text{SiO}_{1.94}$ , can vary from 5.0 to 7.5 eV.<sup>12</sup>

In the present paper, the samples  $\text{SiO}_x$  were prepared at high temperature. In this connection, it is probably the phase separation in  $\text{SiO}_x$  (Fig. 1):  $\text{SiO}_2$ , suboxide, and a—Si. For this reason, to study the short-range of  $\text{SiO}_x$  order, we propose an IM model. Figure 4(a) presents the proposed model of large-scale potential fluctuation caused by variations of the local chemical composition of  $\text{SiO}_x$ , as illustrated by a two-dimensional diagram showing all possible variants of the local (spatial) structure of silicon oxide. The energy band diagram refers to the A-A section. The straight line ( $E=0$ ) indicates the level from which the electron energies are measured (vacuum level). The proposed IM model assumes local spatial fluctuations of the chemical composition of amorphous  $\text{SiO}_x$ . According to the IM model, there is a macroscopic spatial

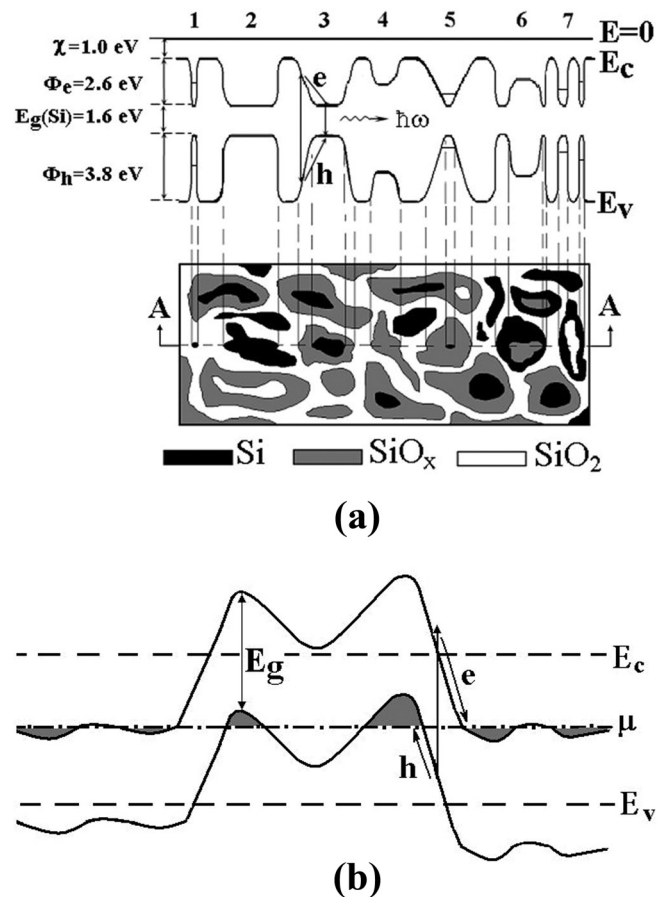


FIG. 4. Schematic diagrams illustrating the intermediate model of  $\text{SiO}_x$ : (a) a two-dimensional diagram of  $\text{SiO}_x$  structure showing the regions of a silicon phase, stoichiometric silicon oxide, and suboxides. The energy band diagram profile of  $\text{SiO}_x$  is in the A-A section. Here,  $E_c$  is the conduction band bottom,  $E_v$  is the valence band top,  $E_g$  is the bandgap width,  $\chi$  is the electron affinity, and  $\Phi_e$  and  $\Phi_h$  are the energy barriers for electrons and holes at the a-Si/ $\text{SiO}_2$  interface, respectively; (b) fluctuations of the Shklovskii-Efros potential in a strongly doped compensated semiconductor ( $\mu$  is the Fermi level).

composition fluctuation in the  $\text{SiO}_x$  which leads to gigantic fluctuations of contra-variant potentials (See Fig. 4(a)) for electrons and holes, i.e., depending on the chemical composition, the bandgap of the  $\text{SiO}_x$  can vary from  $\sim 8$  eV (amorphous  $\text{SiO}_2$ ) to 1.6 eV (amorphous silicon). The barrier of a—Si/ $\text{SiO}_2$  for electrons equals to 2.6 eV because the threshold photoemission of electrons from amorphous silicon equals to one from crystalline silicon. Thereby, the hole fluctuation potential is 3.8 eV. The minimum bandgap width ( $E_g = 1.6$  eV) corresponds to the silicon phase. A decrease in the bandgap width  $E_g$  is suggestive of the presence of suboxides in the silicon oxides matrix. The maximum bandgap width ( $E_g = 8.0$  eV) corresponds to the a— $\text{SiO}_2$  phase.

The IM model assumes smooth variation of the chemical composition at the boundaries between silicon clusters and  $\text{SiO}_2$  matrix. Our experimental data do not allow us to estimate the size of this transition region. Probably, this size may be at the order of several dozens of angstroms. For example, region 1 of Fig. 4(a) corresponds to a “quantum” cluster (with dimensions  $L$  at the order of the de Broglie wavelength of quasi-free electrons in a silicon cluster) incorporated into the  $\text{SiO}_2$  matrix. The ground state energy in this cluster is  $E = \hbar^2/$

$2mL^2$ , where  $m$  is the effective electron mass. Region 2 represents large silicon clusters surrounded by  $\text{SiO}_2$ . In this case, there is no transition layer of suboxides, and the energy band diagram reveals a sharp Si– $\text{SiO}_2$  interface. Large clusters do not feature quantization of the energy levels of electrons and holes. Region 3 is a macroscopic silicon cluster surrounded by a silicon suboxide phase. In this case, the transition from silicon to  $\text{SiO}_2$  in the energy band diagram is smooth. Note, here and below, we assume that the size of the transition region occupied by silicon suboxides is significantly greater than the length of Si–O and Si–Si bonds. Region 4 corresponds to a silicon suboxide cluster in the silicon oxide matrix. Region 5 is a “quantum” silicon cluster incorporated into the suboxide phase, and regions 6 and 7 represent suboxide and oxide clusters, respectively, surrounded by silicon.

The presence of silicon clusters in  $\text{SiO}_x$  is confirmed by Raman scattering data.<sup>13–15</sup> The ESR spectrum of  $\text{SiO}_x$  displays a signal belonging to D – center ( $\bullet\text{Si} \equiv \text{Si}$ ).<sup>16</sup> In Refs. 15 and 17, the photoluminescence was observed from Si nanoclusters and interpreted in terms of band-to-band recombination in Si nanoclusters having the average size of  $\sim 2.5$  nm embedded in  $\text{SiO}_x$ .

The low-frequency dielectric permittivity of  $\text{SiO}_2$  and Si are 3.9 and 11.8, respectively. Therefore,  $\text{SiO}_x$  features spatial fluctuations of the permittivity. The IM model for  $\text{SiO}_x$  charge neutrality is maintained at every point in space. The local electric field for electrons and holes at the same point is different in the magnitude and opposite in its direction. These gigantic contra-variant (for electrons and holes) potential fluctuations will cause non-equilibrium electron/hole pairs moving to the same spatial position with minimum energies, thus favoring their recombination (Fig. 4(a)). In the case of the radiation recombination mechanism,  $\text{SiO}_x$  is an effective radiation medium. Previously, the model of large-scale potential fluctuation was applied to a– $\text{SiN}_x$ .<sup>18</sup>

Figure 4(b) illustrates the Shklovskii-Efros model of large-scale potential fluctuations in a strongly doped compensated semiconductor.<sup>19</sup> According to this model, the bandgap width is constant and the potential fluctuations are caused by the inhomogeneous spatial distribution of charge (ionized) donors and acceptors. Here, the electron-hole pair production is accompanied by spatial separation of electrons and holes, thus not favoring their recombination.

According to the proposed IM model assuming potential fluctuations in  $\text{SiO}_x$ , this material is capable of localizing electrons and holes in potential wells. This property is used in the high performance nonvolatile memory, based on localizing the charge in silicon rich  $\text{SiO}_x$ .<sup>4</sup>

## VI. CONCLUSION

We used x ray photoelectron spectroscopy to study the short-range order in the  $\text{SiO}_x$  layers of variable composition. The  $\text{SiO}_x$  layers were prepared by LP CVD from  $\text{SiH}_4$  and  $\text{N}_2\text{O}$  source at  $750^\circ\text{C}$ . It was established that neither random bonding nor random mixture model can adequately describe the structure of this compound. An intermediate model, according to which the  $\text{SiO}_x$  structure comprises five types of tetrahedral units, is proposed, but the probability of finding a given tetrahedron type is not described by the RB model. It is suggested that fluctuations in the local chemical composition lead to large-scale potential fluctuations.

## ACKNOWLEDGMENTS

This research was supported by the Russian Foundation for Basic Research (Project No. 10-07-00531-a) and Siberian Branch of the Russian Academy of Sciences (Project No. 70).

- <sup>1</sup>M. C. Rossi, S. Salvatori, F. Scrimizzi, F. Galluzzi, R. Janssen, and M. Stutzmann, *J. Lumin.* **80**, 405 (1998).
- <sup>2</sup>I. Z. Indutnyy, P. E. Shepeliavyy, E. V. Michailovskaya, C. W. Park, J. B. Lee, and Y. R. Do, *J. Tech. Phys.* **47**, 720 (2006).
- <sup>3</sup>C. Banerjee, J. Sritharathikhum, A. Yamada, and M. Konagai, *J. Phys. D: Appl. Phys.* **41**, 1 (2008).
- <sup>4</sup>N. V. Duy, S. Jung, K. Kim, D. N. Son, N. T. Nga, J. Cho, B. Choi, and J. Yi, *J. Phys. D: Appl. Phys.* **43**, 1 (2010).
- <sup>5</sup>V. A. Gritsenko, J. B. Xu, R. W. M. Kwok, Y. H. Ng, and I. H. Wilson, *Phys. Rev. Lett.* **81**, 1054 (1998).
- <sup>6</sup>P. Bruesch, T. Stockmeier, F. Stucki, and P. A. Buffat, *J. Appl. Phys.* **73**, 7677 (1993).
- <sup>7</sup>F. G. Bell and L. Ley, *Phys. Rev. B* **37**, 8383 (1988).
- <sup>8</sup>D. V. Tsu, G. Lucovsky, and B. N. Davidson, *Phys. Rev. B.* **40**(3), 1795 (1989).
- <sup>9</sup>I. Berezhinskii, N. V. Sopinskii, and V. S. Khomchenko, *J. Appl. Spectrosc.* **68**, 141 (2004).
- <sup>10</sup>L. Xiao, O. Astakhov, R. Carius, A. Lambert, T. Grundler, and F. Finger, *Phys. Status Solidi C* **7**, 941 (2010).
- <sup>11</sup>V. A. Gritsenko, Yu. G. Shavvalgin, P. A. Pundur, H. Wong, and W. M. Kwok, *Philos. Mag.* **B 80**, 1857 (2000).
- <sup>12</sup>T. W. Hickmott and J. E. Baglin, *J. Appl. Phys.* **50**, 317 (1979).
- <sup>13</sup>Y. Kanzawa, S. Hayashi, and K. Yamamoto, *J. Phys.: Condens. Matter* **8**, 4823 (1996).
- <sup>14</sup>W. L. Zhang, S. Zhang, M. Yang, Z. Liu, Z. H. Cen, T. Chen, and D. Liu, *Vacuum* **84**, 1043 (2010).
- <sup>15</sup>D. Nesheva, C. Raptis, A. Perakis, I. Bineva, Z. Avena, Z. Levi, S. Alexandrova, and H. Hofmeister, *J. Appl. Phys.* **92**, 4678 (2002).
- <sup>16</sup>E. San Andres, A. del Prado, I. Martil, G.G. Diaz, F.L. Martinez, D. Bravo, and F. J. Lopez, *Vacuum* **67**, 531 (2002).
- <sup>17</sup>Y. C. Fang, W. Q. Li, L. J. Qi, L. Y. Li, Y. Y. Zhao, Z. J. Zhang, and M. Lu, *Nanotechnology* **15**, 494 (2004).
- <sup>18</sup>V. A. Gritsenko, D. V. Gritsenko, Yu. N. Novikov, P. B. M. Kwok, and I. Bello, *JETP* **98**, 760 (2004).
- <sup>19</sup>B. I. Shklovskii and A. L. Efros, *Electronic Properties of Doped Semiconductors* (Springer, New York, 1984).